

Lawrence Berkeley National Laboratory

Lawrence Berkeley National Laboratory

Title

Non-diffusive spin dynamics in a two-dimensional electron gas

Permalink

<https://escholarship.org/uc/item/6966q5n3>

Authors

Weber, Christopher P.
Orenstein, Joseph
Bernevig, B. Andrei
[et al.](#)

Publication Date

2006-12-12

Peer reviewed

Non-diffusive spin dynamics in a two-dimensional electron gas

C.P. Weber^{1,*}, J. Orenstein¹, B. Andrei Bernevig², Shou-Cheng Zhang², Jason Stephens³, and D.D. Awschalom³

¹*Physics Department, University of California, Berkeley and*

Materials Science Division, Lawrence Berkeley National Laboratory, Berkeley, CA 94720

²*Physics Department, Stanford University, Stanford, CA 94305*

³*Center for Spintronics and Quantum Computation,
University of California, Santa Barbara, California 93106, USA*

(Dated: October 3, 2006)

We describe measurements of spin dynamics in the two-dimensional electron gas in GaAs/GaAlAs quantum wells. Optical techniques, including transient spin-grating spectroscopy, are used to probe the relaxation rates of spin polarization waves in the wavevector range from zero to $6 \times 10^4 \text{ cm}^{-1}$. We find that the spin polarization lifetime is maximal at nonzero wavevector, in contrast with expectation based on ordinary spin diffusion, but in quantitative agreement with recent theories that treat diffusion in the presence of spin-orbit coupling.

PACS numbers: 42.65.Hw, 72.25.b, 75.40.Gb.

Electronic systems with strong spin-orbit interaction (SOI) exhibit exotic effects that arise from the coupling of spin polarization and charge current, such as spin Hall currents^{1,2,3,4,5,6,7} and current-induced spin polarization⁸. These effects involve manipulation of the electron spin via electric, rather than magnetic, fields, creating the potential for applications in areas from spintronics to quantum computing⁹. However, SOI is a double-edged sword, as it also has the undesired effect of causing decay of spin polarization, reflecting the non-conservation of the total spin operator, \vec{S} , i.e. $[\vec{S}, \mathcal{H}] \neq 0$, where \mathcal{H} is any Hamiltonian that contains spin-orbit coupling.

In the consideration of spin-orbit coupled systems, a great deal of attention has been focused on quantum wells or heterostructures fabricated in III-V semiconductors, where breaking of inversion symmetry allows coupling that is linear in momentum. For electrons propagating in [001] planes, the most general form of the linear coupling includes both Rashba¹⁰ and Dresselhaus¹¹ contributions:

$$\mathcal{H}_{so} = \alpha(k_y\sigma_x - k_x\sigma_y) + \beta(k_x\sigma_x - k_y\sigma_y), \quad (1)$$

where $k_{x,y}$ is the electron wavevector along the [10], [01] directions in the plane, and α and β are the strengths of the Rashba and Dresselhaus couplings. The spin-orbit terms generate an effective in-plane magnetic field, \vec{b}_{so} , whose direction depends on \vec{k} . Spin nonconservation takes the form of precession, at a rate governed by $\vec{b}_{so}(\vec{k})$, during an electron's free flight between collisions. In the Dyakanov-Perel (DP) regime¹², where the precession angle during the free-flight time τ is small, a spatially uniform spin polarization will relax exponentially to zero at the rate $1/\tau_s \propto |\vec{b}_{so}|^2\tau$. Although this process relaxes the initial polarization state, spin memory is not entirely lost, even after the electron undergoes many collisions. The relationship between real-space trajectory and spin precession leads to a correlation between the electron's position and its spin. Such correlations are predicted to enhance the lifetime of certain spatially inhomogeneous

spin polarization states beyond what would be expected for conventional spin diffusion¹³.

Burkov *et al.*¹³ considered \mathcal{H}_{so} with only Rashba coupling ($\beta = 0$), and showed that a helical spin density wave with wavevector $\sqrt{15}m\alpha/2$ decays more slowly than a uniform (or $q = 0$) spin polarization, by a factor 32/7. This contrasts with ordinary spin diffusion, where the decay rate of a polarization wave increases monotonically ($\propto q^2$) with increasing wavevector. More recently, Bernevig *et al.*¹⁴ showed that the lifetime of the spin helix is enhanced further in the presence of both Rashba and Dresselhaus coupling, and diverges as $\alpha \rightarrow \beta$. The infinite lifetime, or "persistent spin helix" (PSH) state, is a manifestation of an exact $SU(2)$ symmetry of \mathcal{H}_{so} at the point $\alpha = \beta$. As a consequence of the $SU(2)$ symmetry, a spiral spin polarization in the z, x_+ plane (where \hat{z} and \hat{x}_+ are the normal and [11] directions, respectively) with wavevector $4m\alpha\hat{x}_+$ is a conserved quantity. These predictions suggest the possibility of manipulating spin polarization through SOI, without necessarily compromising spin memory, by controlling α/β with externally applied electric fields.

Transient spin grating (TSG) experiments^{15,16} are particularly well-suited to testing the theoretical predictions of Refs.^{13,14}, as they directly probe the decay rate of nonuniform spin distributions. In the TSG technique, a spatially periodic polarization of the out-of-plane spin, S^z , is created by a pair of interfering ultrashort laser pulses. By varying the relative angle of the two pump beams, we are able to vary the magnitude of the grating wavevector \vec{q} in the range $0.44 - 5.3 \times 10^4 \text{ cm}^{-1}$, corresponding to wavelengths in the range from $\approx 1 - 15$ microns. The subsequent time evolution of the spin polarization wave amplitude, $S_q^z(t)$, is measured by coherent detection of a time-delayed probe beam that diffracts from the photoinjected "spin grating."

In this work we report detailed TSG measurements on two samples, each consisting of 30 quantum wells of thickness 120 Å. One was with δ -doped with Si in the barriers to create a high mobility ($\mu \simeq 150,000 \text{ cm}^2/\text{V-s}$

at 5 K) two-dimensional electron gas (2DEG) with carrier density $7.8 \times 10^{11} \text{ cm}^{-2}$. The δ layers are symmetrically located on either side of each well. The second sample is identical except that the mobility of the electrons was reduced to $\simeq 3,500 \text{ cm}^2/\text{V}\cdot\text{s}$ by placing 83% of the dopant atoms in the wells, rather than in the barriers.

The TSG measurements show that the lifetime of S_q^z is maximal at nonzero $|\vec{q}|$ in both samples, in contrast to expectations for simple diffusion but in agreement with the prediction of Burkov *et al.*¹³. The magnitude of the lifetime enhancement and its dependence on the direction of \vec{q} point to the presence of both Rashba and Dresselhaus interactions in our samples. Quantitative agreement between the theory of Bernevig *et al.*¹⁴ and our experimental results suggests the feasibility of realizing and detecting a PSH in samples engineered to achieve $\alpha \approx \beta$.

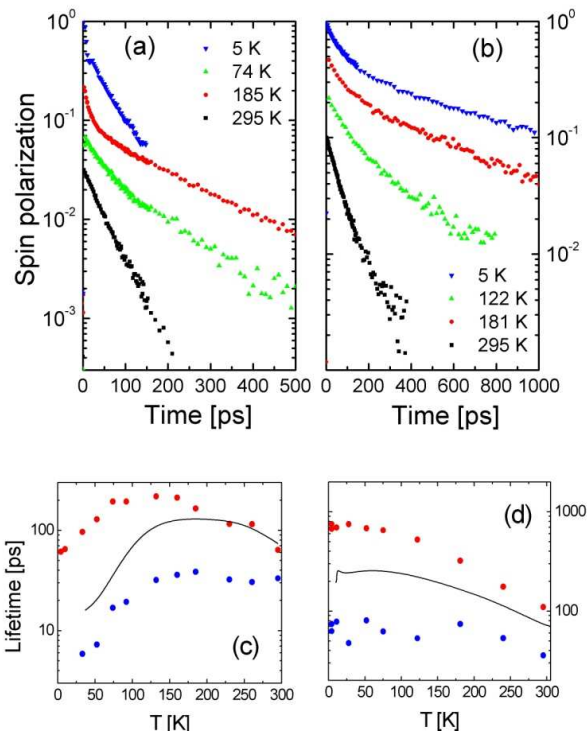


FIG. 1: [Color Online] Decay of the out-of-plane component of spin polarization wave with wavevector in the [11] direction, for (a) the high-mobility sample with $|\vec{q}| = 0.58 \times 10^4 \text{ cm}^{-1}$ and (b) the low-mobility sample with $|\vec{q}| = 0.69 \times 10^4 \text{ cm}^{-1}$, for several temperatures. The initial value of spin polarization is estimated at a few percent for all measurements. Decay curves are offset vertically for clarity. Solid symbols in panels (c) and (d) indicate the temperature dependence of the two time constants obtained from a double exponential fit to the decay curves. Solid lines are the lifetime of a spatially uniform spin polarization.

Panels (a) and (b) of Fig. 1 show the decay of $S_q^z(t)$ for the high- μ and low- μ samples, respectively, measured at the wavevectors where the decay rate is smallest. In both samples the decay of the grating is clearly not a sin-

gle exponential at low T and crosses over to nearly single exponential as room temperature is approached. All the decay curves can be fitted to a double exponential form, $a_1 \exp(-t/\tau_1) + a_2 \exp(-t/\tau_2)$, with equal weighting factors ($a_1 = a_2$) over almost the entire range of T . The only exception is the $T < 25 \text{ K}$ regime of the high- μ sample, where the momentum relaxation rate, $1/\tau$, becomes comparable to the spin precession frequency, Ω . In this ($\Omega\tau \geq 1$) regime the initial decay is damped oscillatory rather than exponential¹⁶. The solid symbols in panels (c) and (d) are the time constants τ_1 and τ_2 extracted from the double-exponential fit, plotted as a function of T . For both samples the ratio between the fast and slow rates is at least a factor of ten at low T and gradually diminishes as T approaches room temperature. The solid lines are the lifetimes of the uniform spin polarization, $\tau_s(T)$, as obtained from decay of transient Faraday rotation induced by a single, circularly polarized pump beam. For all temperatures, the $q = 0$ polarization decays as a single exponential, whose lifetime lies between the two lifetimes observed at nonzero q .

The dispersion of the decay rates with $|\vec{q}|$ [11] is shown in Figs. 2(a) and 2(b), for the high and low μ samples, respectively. We present results for $T = 50 \text{ K}$, a temperature at which both samples are in the $\Omega\tau < 1$ regime, and yet the ratio τ_2/τ_1 remains large (in a certain range of q). For both samples, the larger of the two time constants peaks sharply at $|\vec{q}| \approx 0.6 \times 10^4 \text{ cm}^{-1}$. The lifetime of the more rapidly decaying component decreases monotonically with increasing $|\vec{q}|$, consistent with simple diffusion.

The spin-dynamical effects illustrated in Figs. 1 and 2, biexponential decay and non-monotonic dispersion, are in quantitative agreement with the theory of coupled charge and spin dynamics in the presence of \mathcal{H}_{so} , which we describe briefly below. Assuming a single, isotropic τ , Burkov *et al.*¹³ and Bernevig *et al.*¹⁴ derived a set of four equations that describes the coupling of electron density $n_q(t)$ and the three components of $\vec{S}_q(t)$ brought about by the SOI. Along the [11] and $[1\bar{1}]$ directions, the four equations separate into two coupled pairs. For $\vec{q} \parallel [11]$, spin precesses in the $z - x_+$ plane, leading to coupling of S^{x+} and S^z .

Solving the pair of equations that couple S^z and S^{x+} yields two eigenmodes and corresponding eigenfrequencies $i\omega_{1,2}(q) \equiv 1/\tau_{1,2}(q)$. The $\vec{q} \parallel [11]$ eigenfrequencies are,

$$\frac{1}{\gamma_0\tau(q)} = \frac{q^2}{2q_0^2} + 3 + \sin 2\phi \pm \sqrt{(1 - \sin 2\phi)^2 + \frac{4q^2}{q_0^2}(1 + \sin 2\phi)}, \quad (2)$$

where $q_0 \equiv m^*v_{so}/\hbar$ is the reciprocal of the distance required for an electron to precess by 2π in the spin-orbit field and $\gamma_0 \equiv v_{so}^2 k_F^2 \tau$ is the typical DP (*i.e.*, $q = 0$) decay rate. The parameters $\phi \equiv \tan^{-1}(\alpha/\beta)$ and

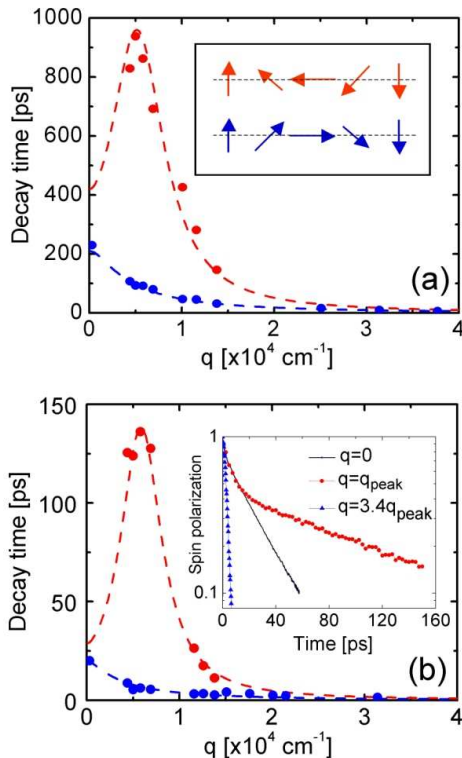


FIG. 2: [Color Online] Decay lifetimes obtained from best fit of a double exponential to experimentally measured decay of spin polarization, as a function of wavevector \vec{q} parallel to the [11] crystal axis. Data are shown for the (a) low- μ and (b) high- μ samples, at 50 K. The dashed lines are fits to a theory (described in the text) in which the two lifetimes correspond to the positive and negative spin helices illustrated in Fig. 2(a) inset. Fig. 2(b) inset: Comparison of spin polarization decay at $q = 0$, $0.58 \times 10^4 \text{ cm}^{-1}$, and $2.01 \times 10^4 \text{ cm}^{-1}$.

$v_{so} \equiv \sqrt{\alpha^2 + \beta^2}$ reflect the relative and combined coupling strengths of the Rashba and Dresselhaus interactions, respectively. Finally, the spin diffusion coefficient $D_s \equiv v_F^2 \tau / 2$ is given by $\gamma_0 / 2q_0^2$.

The solutions for $\vec{q} \parallel [11]$ are especially interesting at the $SU(2)$ point where $\alpha = \beta$, and $\sin 2\phi = 1$. In this case the eigenvectors are $(1, \pm i) / \sqrt{2}$, corresponding to forward and backward spin spirals in the z, x_+ plane, for each value of q . A TSG experiment creates the initial condition $(1, 0)$, which couples with equal strength to the two eigenvectors. The subsequent time evolution of the two eigenmodes has the form of a double exponential decay with equal weighting factors. At the “resonant” wavevector $q_0 \sqrt{8}$, the two decay rates are 0 and $16\gamma_0$. After decay of the unstable eigenmode, the PSH remains stable, despite the rapid electron scattering and spin precession that are occurring. The eigenfrequencies for $\vec{q} \parallel [11]$ can be obtained from Eq. 2 as well, if we replace ϕ by $-\phi$. At the same $SU(2)$ point where the PSH exists for $\vec{q} \parallel [11]$, the spin dynamics for $\vec{q} \parallel [1\bar{1}]$ obey simple diffusion.

Several features of the physics at the $SU(2)$ point remain when $\alpha \neq \beta$, but both are nonzero. The lifetime at the resonant wavevector is enhanced relative to the case when only one of two interactions is present, although it no longer diverges. The enhancement is expected to be stronger for $\vec{q} \parallel [11]$ than $\vec{q} \parallel [1\bar{1}]$. The eigenvectors are still admixtures of S^z and S^{x+} and the photoinjected wave of pure S^z will again decay as a double exponential. However, the weighting factors are q -dependent and the long-lived state will be an elliptical, rather than circular, spin helix.

With this overview of the theory, we return to the experimental data. The dotted lines in Fig. 2 show the best fits obtained by varying parameters in Eq. 2. The fits yield parameter values $v_{so} = 460 \text{ m/s}$, $\phi = 0.2$, and $D_s = 1000 \text{ cm}^2/\text{s}$ for the higher- μ sample and $v_{so} = 480 \text{ m/s}$, $\phi = 0.08$, and $D_s = 105 \text{ cm}^2/\text{s}$ for the intentionally disordered sample. The above value of v_{so} for the high- μ sample predicts a spin-precession frequency for ballistic electrons, $\Omega = v_{so} k_F = 0.10 \text{ THz}$, that is within 10% of the experimental value¹⁷. The theory applies equally well to both samples, despite a difference of about ten in their scattering rates. Note that smaller τ leads to smaller spin relaxation rates, as the entire dispersion scales with the DP relaxation rate, $4\gamma_0$.

A surprising feature of the theory¹⁴ is the sensitivity of the dispersion curves to small admixtures of Rashba coupling into a pure Dresselhaus system, or *vice versa*. Our quantum wells are designed to be perfectly symmetric and therefore no Rashba term is expected. However, the maximum lifetime enhancement, ~ 7 , for the higher μ sample is significantly larger than the factor $32/7$ predicted for $\alpha = 0$. This discrepancy is accounted for by a relatively small admixture $\alpha \simeq 0.2\beta$. It is possible that the presence of a small Rashba contribution can be traced differences in the interface on either side of the well, a known feature of the GaAs/GaAlAs system^{18,19}. It is interesting that the value $\alpha/\beta \simeq 0.08$ is smaller in the lower- μ sample. The difference may reflect the tendency of the ionized impurities to attract electrons toward the barrier in case of δ -doping, as opposed to doping inside the well.

A further prediction of the theory is that even small α/β generates a large anisotropy in the dispersion curves. To test this prediction we measured S_q^z at 50 K in the higher- μ sample, for \vec{q} oriented along the [11], $[1\bar{1}]$, and $[10]$ directions. The results shown in Fig. 3 demonstrate that the lifetime enhancement is strong for $\vec{q} \parallel [11]$ and weak for $\vec{q} \parallel [1\bar{1}]$. The line through the [11] curve is calculated using Eq. 2 for the lifetimes and Eq. 22 of Ref.¹⁴ for the weighting factors of the double exponential decay. The parameters are the same as used to fit the dispersion along [11]. The weighting factors and decay rates for $\vec{q} \parallel [1\bar{1}]$ are calculated using the *same parameters*, provided that we replace ϕ by $-\phi$. The theory is clearly quite successful in providing a quantitative description of the spin relaxation dynamics seen in our experiment.

The only feature of the data not captured by the the-

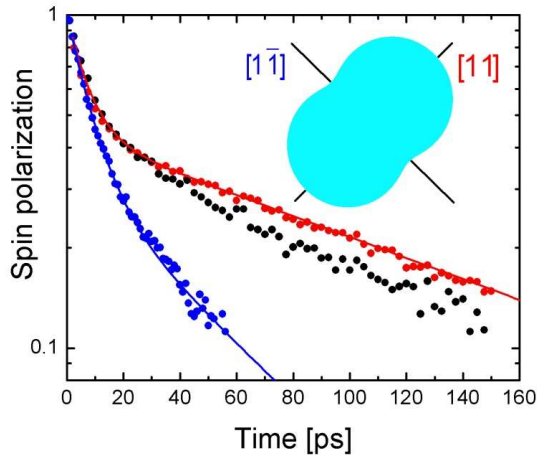


FIG. 3: [Color Online] Decay of spin polarization in the high- μ sample as a function of time for three orientations of the grating wavevector (top-to-bottom: $[11]$, $[10]$, and $[1\bar{1}]$). The lines through the data are predictions of the theory described in the text, using the parameters that were obtained from fitting the dispersion curves. The anisotropy is smaller in the low- μ sample, which is consistent with the conclusion based on the dispersion data. **Inset:** Fermi contour for a system of free electrons subject to the SOI described by Eq. 1, showing the origin of the extremal orientations. Rashba coupling set to one-half of Dresselhaus (larger than in the systems under study here) for the purpose of illustration.

ory described above is the gradual decrease in the τ_2/τ_1 ratio with increasing T (shown in Fig. 1) that takes place for both samples. The characteristic scale of T clearly is not the spin-orbit splitting, which is $\sim v_F q_0$ or about 1 K for our samples. We speculate that the T -dependence of τ_2/τ_1 is a consequence of the cubic (in k) Dresselhaus coupling, $\mathcal{H}_{cD} \propto k_x k_y^2 \sigma_x - k_y k_x^2 \sigma_y$, which does not appear in Eq. 1. \mathcal{H}_{cD} is non-negligible when $\langle k_z^2 \rangle$, the expectation value of k_z^2 in the lowest subband, becomes comparable to k_F^2 . The cubic Dresselhaus coupling destroys the proportionality $\Omega \propto k$, which ensures that the precession angle in a free-flight between collisions depends only on the electron's displacement, and not on its velocity. In the presence of \mathcal{H}_{cD} the precession angle will depend

on k , and the fractional spread in precession angle for a given Δk is $\sim k_F \Delta k / \langle k_z^2 \rangle$. Assuming a thermally induced momentum distribution $\Delta k \sim T/v_F$, the relative variation in precession angle is $\sim T/E_1$, the ratio of the temperature to the energy of the first excited subband. Our results are consistent with E_1 (which is ≈ 500 K for our samples) as the characteristic energy scale above which the correlations that generate the PSH are lost.

Finally, we discuss directions for future research that are suggested by the conclusions of this work. The main implication of the theory and experiments described above is that $SU(2)$ spin symmetry can be recovered, despite the presence of SOI, if the condition $\alpha = \beta$ can be satisfied. This can be accomplished by increasing the strength of the Rashba interaction, as compared with our samples, by designing asymmetric doping and/or barrier profiles, or by applying a gate electrode. Once achieved, the $SU(2)$ symmetry is robust with respect to disorder and interactions¹⁴, and could be stabilized at room temperature by increasing E_1 . Schliemann *et al.*²⁰ previously discussed some attractive features of a system in which $\alpha = \beta$ for logic devices based on spin transport. They described a device structure in which spin is injected and detected at two points, and showed that if $\alpha = \beta$ the change in direction of the injected spin depends only on the vector displacement, \vec{a} , of the two point contacts, even in the presence of strong scattering. Modulating the Rashba coupling via an external gate can then destroy the long-range spin correlation. The restriction to point contacts is actually unnecessary in the $SU(2)$ system because the net spin precession depends only on the projection of \vec{a} onto \hat{x}_+ . For example, spin injected with arbitrary polarization from anywhere along a line contact defined by $x_+ = 0$ will be detected with the same spin anywhere along a line contact at $x_+ = n\pi/2m\alpha$, where n is an integer. Thus, in principle, a planar spin logic device operating at room temperature is feasible, if highly spin selective contacts to the 2DEG can be fabricated.

B.A.B. wishes to acknowledge the hospitality of the Kavli Institute for Theoretical Physics at University of California at Santa Barbara, where part of this work was performed. This work is supported by the NSF through the grants DMR-0342832, DMR-0305223, and by the US Department of Energy, Office of Basic Energy Sciences under contract DE-AC03-76SF00515.

* Electronic address: cpweber@lbl.gov

¹ M. I. D'yakonov and V. I. Perel', Phys. Lett. A **35**, 459 (1971).

² J. Hirsch, Phys. Rev. Lett. **83**, 1834 (1999).

³ S. Murakami, N. Nagaosa, and S. Zhang, Science **301**, 1348 (2003).

⁴ J. Sinova *et al.*, Phys. Rev. Lett. **92**, 126603 (2004).

⁵ Y. K. Kato, R. C. Myers, A. C. Gossard, and D. D. Awschalom, Science **306**, 1910 (2004).

⁶ J. Wunderlich, B. Kaestner, J. Sinova, and T. Jungwirth, Phys. Rev. Lett. **94**, 047204/1 (2005).

⁷ V. Sih *et al.*, Nature Physics **1**, 31 (2005).

⁸ Y. K. Kato, R. C. Myers, A. C. Gossard, and D. D. Awschalom, Phys. Rev. Lett. **93**, 176601 (2004).

⁹ S. A. Wolf *et al.*, Science **294**, 1488 (2001).

¹⁰ Y. A. Bychkov and E. I. Rashba, J. Phys. C **17**, 6039 (1984).

¹¹ G. Dresselhaus, Phys. Rev. **100**, 580 (1955).

- ¹² M. I. D'yakonov and V. I. Perel', Sov. Phys. Solid State **13**, 3023 (1972).
- ¹³ A. A. Burkov, A. S. Nunez, and A. H. MacDonald, Phys. Rev. B **70**, 155308 (2004).
- ¹⁴ B. A. Bernevig, J. Orenstein, and S.-C. Zhang, Condmat/0606196 (2006).
- ¹⁵ A. R. Cameron, P. Riblet, and A. Miller, Phys. Rev. Lett. **76**, 4793 (1996).
- ¹⁶ C.P. Weber *et. al*, Nature **437**, 1330 (2005).
- ¹⁷ C. Weber, PhD Thesis, Department of Physics, University of California, Berkeley, Berkeley, CA 94720 (2005), IBNL Document 59144.
- ¹⁸ W. Braun, A. Trampert, L. Däweritz, and K. H. Ploog, Phys. Rev. B **55**, 1689 (1997).
- ¹⁹ E. A. de Andrada e Silva, G. L. Rocca, and F. Bassani, Phys. Rev. B **55**, 16293 (1997).
- ²⁰ J. Schliemann, J. C. Egues, and D. Loss, Phys. Rev. Lett. **90**, 146801 (2003).